Spin transport in magnetic multilayers

2007 J. Phys.: Condens. Matter 19 356204

(http://iopscience.iop.org/0953-8984/19/35/356204)

IOP PUBLISHING JOURNAL OF PHYSICS: CONDENSED MATTER

J. Phys.: Condens. Matter **19** (2007) 356204 (14pp) doi:10.1088/0953-8984/19/35/356204

Spin transport in magnetic multilayers

K Akabli, H T Diep[1] and S Reynal[2]

Laboratoire de Physique Théorique et Modélisation, CNRS-Université de Cergy-Pontoise, UMR 8089, 2, Avenue Adolphe Chauvin, 95302 Cergy-Pontoise Cedex, France

E-mail: diep@u-cergy.fr

Received 7 May 2007, in final form 6 July 2007
Published 2 August 2007
Online at stacks.iop.org/JPhysCM/19/356204

Abstract

We study by extensive Monte Carlo simulations the transport of itinerant spins travelling inside a multilayer composed of three ferromagnetic films antiferromagnetically coupled to each other in a sandwich structure. The two exterior films interact with the middle one through non-magnetic spacers. The spin model is the Ising one and the in-plane transport is considered. Various interactions are taken into account. We show that the current of the itinerant spins going through this system depends strongly on the magnetic ordering of the multilayer: at temperatures T below (above) the transition temperature T_c, a strong (weak) current is observed. This results in a strong jump of the resistance across T_c. Moreover, we observe an anomalous variation, namely a peak, of the spin current in the critical region just above T_c. We show that this peak is due to the formation of domains in the temperature region between the low-T ordered phase and the true paramagnetic disordered phase. The existence of such domains is known in the theory of critical phenomena. The behaviour of the resistance obtained here is compared to a recent experiment. An excellent agreement with our physical interpretation is observed. We also show and discuss the effects of various physical parameters entering our model, such as interaction range, strength of electric and magnetic fields and magnetic film and non-magnetic spacer thicknesses.

1. Introduction

The so-called giant magnetoresistance (GMR) effect was discovered experimentally 20 years ago by Fert and co-workers [1] and by Grunberg [2]. Since then, intensive investigations, both experimentally and theoretically, have been carried out to understand the origin and the behaviour of the spin current in magnetic multilayer systems [3–9]. This spectacular development is due mainly to an important number of industrial applications using such systems in data storage and magnetic sensors [3, 4].

[1] Author to whom any correspondence should be addressed.
[2] Permanent address: ENSEA, 6, Avenue du Ponceau, 95014 Cergy-Pontoise Cedex, France.

Experimental observations show that when the spin of an itinerant spin is parallel to the spins of the environment it will go through easily while it will be stopped if it encounters an antiparallel spin medium. The resistance is stronger in the latter case resulting in GMR. Although many theoretical investigations have been carried out, detailed understanding of the influence of each physical parameter on the spin current is still lacking. For example, the role of interface scattering and the effect of interface roughness on the GMR are still currently being investigated (see for example [6, 7] and references therein). In addition, to date no Monte Carlo (MC) simulations have been performed regarding the temperature dependence of the dynamics of spins participating in the current. This defines the aim of this work.

This paper deals with the transport of spins in a system composed of three magnetic films. We show that the spin current depends on the orientation of the lattice spins found on the trajectory. The dependence of the spin transport on the magnetic ordering, i.e., on the temperature, is studied. The difficulty of the task is that we have to deal at the same time with surface and interface effects and with dynamical properties of itinerant spins interacting with the lattice spins. The surface physics of systems such as films and multilayers has been studied a great deal at equilibrium during the last 30 years. This was motivated in particular by applications in magnetic recording, let alone fundamental theoretical interests. Much is understood theoretically and experimentally in thin films whose surfaces are 'clean', i.e., contain no impurities, no steps etc [10–15]. Far less is known—at least theoretically—on complicated thin films with special surface conditions such as defects, arrays of dots and magnetization reversal phenomena. As a result, studying the behaviour of itinerant electrons injected into such systems is a formidable task which cannot be fulfilled in every respect.

The paper is organized as follows. Section 2 is devoted to the description of our model and the rules that govern its dynamics. We take into account (i) interactions between itinerant and lattice spins, (ii) interactions between itinerant spins themselves, and (iii) interactions between lattice spins. Where rules governing the dynamics are concerned, we include a thermodynamic force due to the gradient of itinerant spin concentration, an applied electric field that drives electrons, and the effect of a magnetic field. In section 3, we describe our MC method and discuss the results we obtained for several physical quantities in various situations, e.g., the mean free path, the spin current and the resistance. Comparison with a very recent experiment [16] performed on a permalloy–insulator multilayer is also shown in this section. Concluding remarks are given in section 4.

2. Model

2.1. Interactions

We consider in this paper three ferromagnetic films being antiferromagnetically coupled to each other via non-magnetic layers. We use the Ising model and the face-centred cubic (FCC) lattice for the films. The system is shown in figure 1, where the films are stacked along the z direction.

The multilayer is made up of three films, each of which has a volume given by $N_x \times N_y \times N_z$, where N_z denotes the number of atomic layers (i.e., single film thickness). Periodic boundary conditions are used in the xy planes. Non-magnetic spacers sandwiched between films have a thickness d.

Spins at FCC lattice sites are called 'lattice spins' hereafter. They interact with each other through the following Hamiltonian:

$$\mathcal{H}_l = -\sum_{\langle i,j \rangle} J_{i,j} \mathbf{S}_i \cdot \mathbf{S}_j, \tag{1}$$

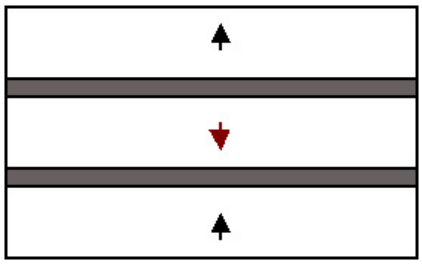

Figure 1. Ground-state spin configuration. Thick arrows indicate the spin orientations. Non-magnetic spacers are black.

(This figure is in colour only in the electronic version)

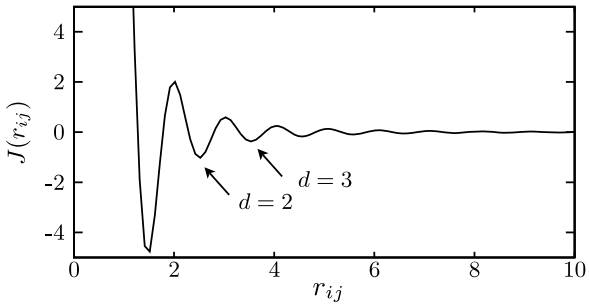

Figure 2. The RKKY interaction for two spins across the non-magnetic layer is shown as a function of their distance r_{ij}. $J_0 = 16.6$ and $\alpha = 6.18$ have been used so that $J_{i,j} = -1.005$ for non-magnetic spacer thickness $d = 2$.

where $\mathbf{S}_i$ is the Ising spin at lattice site i, and $\sum_{\langle i,j\rangle}$ indicates the sum over every nearest-neighbour (NN) spin pair $(\mathbf{S}_i, \mathbf{S}_j)$. For simplicity, we will consider the case where all exchange interactions $J_{i,j}$ are ferromagnetic and equal to $J(>0)$, except for the interaction across the non-magnetic spacer which we define using the following Rudermann–Kittel–Kasuya–Yosida (RKKY) model:

$$J_{i,j} = J_0 \frac{\cos(\alpha r_{ij})}{r_{ij}^3}. \tag{2}$$

Here, i and j refer to spins on either side of a non-magnetic layer, and J_0 and α are constants chosen in such a way that the strength of $J_{i,j}$ is physically reasonable. The shape of the interaction is sketched in figure 2.

When the coupling across non-magnetic layers is antiferromagnetic, the ground state corresponds to the two exterior films having spins pointing in one direction and the interior one spins pointing in the opposite direction. Note that the RKKY interaction is used here for the interaction in the z direction across the non-magnetic spacers. This interaction allows the interaction to change its sign (ferromagnetic to antiferromagnetic or vice versa) when the spacer thickness in the z direction varies. In the perpendicular transport (CPP configuration defined below), this interaction will affect the current behaviour, but in the parallel transport (CIP) studied here, it does not play an important role since the spins move in the x direction.

In order to study the spin transport inside the multilayer system described above, we consider a flow of itinerant spins interacting with each other and with the lattice spins. The

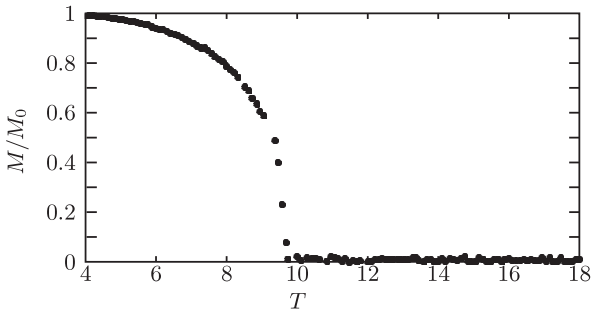

Figure 3. Total staggered lattice magnetization versus temperature T. M_0 is the ground-state staggered lattice magnetization. T_c is $\simeq$9.75 in units of $J = 1$.

interaction between itinerant spins is defined as follows:

$$\mathcal{H}_m = -\sum_{\langle i,j\rangle} K_{i,j}\mathbf{s}_i \cdot \mathbf{s}_j, \tag{3}$$

where $\mathbf{s}_i$ is the Ising spin at position $\vec{r}_i$, and $\sum_{\langle i,j\rangle}$ denotes a sum over every spin pair $(\mathbf{s}_i, \mathbf{s}_j)$. The interaction $K_{i,j}$ depends on the distance between the two spins, i.e., $r_{ij} = |\vec{r}_i - \vec{r}_j|$. A specific form of $K_{i,j}$ will be chosen below. The interaction between itinerant spins and lattice spins is given by

$$\mathcal{H}_r = -\sum_{\langle i,j\rangle} I_{i,j}\mathbf{s}_i \cdot \mathbf{S}_j, \tag{4}$$

where the interaction $I_{i,j}$ depends on the distance between the itinerant spin $\mathbf{s}_i$ and the lattice spin $\mathbf{S}_i$. For the sake of simplicity, we assume the same form for $K_{i,j}$ and $I_{i,j}$, namely,

$$K_{i,j} = K_0 \exp(-r_{ij}) \tag{5}$$

$$I_{i,j} = I_0 \exp(-r_{ij}), \tag{6}$$

where K_0 and I_0 are constants expressing the respective strength of interactions.

2.2. Dynamics

Let us now explain the procedure we utilize in our simulation. First we study the thermodynamic properties of the multilayer system alone, i.e., without itinerant spins, using equation (1). In this view, we perform MC simulations in order to determine quantities such as the internal energy, the specific heat, layer magnetizations, and the susceptibility as functions of temperature T [17]. From these physical quantities we determine the critical temperature T_c below which the system is in the ordered phase, e.g., with up-spin phase for the outer films and down-spin phase for the middle film. The total staggered lattice magnetization is defined as $M = (M_1 - M_2 + M_3)/3$, where M_i $(i = 1, 2, 3)$ is the magnetization of the ith film. We depict in figure 3 the lattice magnetization versus T.

Figure 4 shows the susceptibility calculated from the fluctuations of M for two spacer thicknesses $d = 2, 3$. T_c is equal to $\simeq$9.75 and $\simeq$9.49 respectively for these spacers.

Once the lattice has been equilibrated at T, we study the dynamics of itinerant spins at that temperature by injecting N itinerant spins into the multilayer system. There are two ways of doing this: (i) the itinerant spins move parallel to the film surface (CIP case); (ii) the itinerant spins move perpendicular to the films (CPP case). In this paper we show results in the CIP case.

The itinerant spins in the CIP case move into the system at one end, travel in the x direction, and escape the system at the other end to reenter again at the first end under periodic boundary

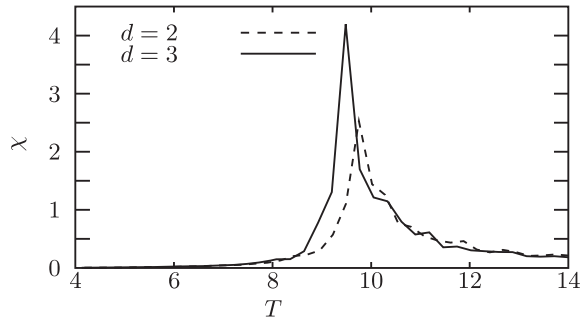

Figure 4. Susceptibility χ of staggered lattice magnetization versus temperature T for two spacer thicknesses $d = 2$ (dashed line) and $d = 3$ (solid line).

conditions (PBC). Note that PBC are used to ensure that the average density of itinerant spins remains constant during the time (stationary regime). The dynamics of itinerant spins is governed by the following interactions:

(i) An electric field **E** is applied in the x direction. Its energy is given by

$$\mathcal{H}_{\mathrm{E}} = -\mathbf{E} \cdot \mathbf{v}, \tag{7}$$

where **v** is the velocity of the itinerant spin.

(ii) A chemical potential term which depends on the concentration of itinerant spins within a sphere of radius D_2 ('concentration gradient' effect). Its form is given by

$$\mathcal{H}_{\mathrm{c}} = Dn(\mathbf{r}), \tag{8}$$

where $n(\mathbf{r})$ is the concentration of itinerant spins in a sphere of radius D_2 centred at **r**. D is a constant taken equal to K_0 for simplicity.

(iii) Interactions between a given itinerant spin and lattice spins inside a sphere of radius D_1 (equation (4)).

(iv) Interactions between a given itinerant spin and other itinerant spins inside a sphere of radius D_2 (equation (3)).

Let us first consider the case without an applied magnetic field.

The simulation is carried out as follows. At a given T we calculate the energy of an itinerant spin by taking into account all the interactions described above. Then we tentatively move the spin under consideration to a new position with a step of length v in an arbitrary direction, taken from a Gaussian distribution centred at v_0 with width Δ. Note that this move is immediately rejected if the new position is inside a sphere of radius r_0 centred at a lattice spin or an itinerant spin. This excluded space emulates the Pauli exclusion principle on the one hand, and the interaction with lattice phonons on the other. For the sake of example, if the spacing between NN lattice spins is $\sqrt{2}$ then r_0 is taken of the order of 0.05. This value can be made temperature dependent to account for the cross section of phonon–electron collisions.

If the new position does not lie in a forbidden region of space, then the move is accepted with a probability given by the standard Metropolis algorithm [17]; in particular, it is always accepted if the energy of the itinerant spin at the new position is lower than its previous value.

3. Monte Carlo results

In this section, we show the results obtained by MC simulations with the Hamiltonians given above. All Ising spins are of magnitude $s = S = 1$.

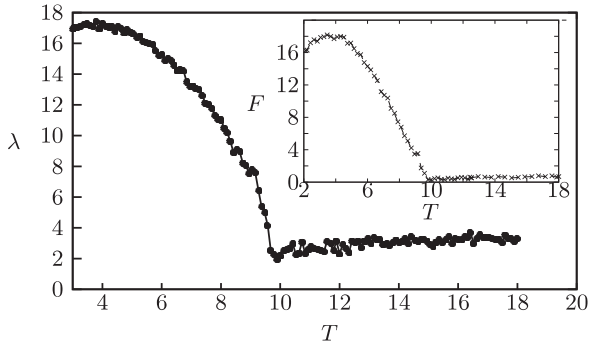

Figure 5. Characteristic distance λ travelled by an itinerant spin during 100 MC steps versus T. Inset: mean free path F versus T. λ and F are in units of the FCC cell length.

The parameters we use in most calculations are, except otherwise stated, $N_x = 36$, $N_y = 10$ and $N_z = 5$ for the dimension of the films, and $d = 2$ for the spacer thickness. We also make use of PBC in the xy plane.

At each temperature the equilibration time for the lattice spins lies around 10^6 MC steps per spin and we compute statistical averages over 10^6 MC steps per spin. Taking $J = 1$, we obtain $T_c \simeq 9.75$ for the estimate of the critical temperature of the lattice spins (see figures 3 and 4). Before calculating the spin current, we let N itinerant spins travel through the system several thousands times until a steady state is reached. The parameters used for the results shown below are $D_1 = D_2 = 1$ (in units of the FCC cell length), $K_0 = I_0 = 2$, $N = 1500$, $v_0 = 1$, $\Delta = 0.1$, $r_0 = 0.05$.

In figure 5 we sketch the travelling length λ computed after a fixed lapse of time as a function of temperature T. Let us call λ hereafter the 'characteristic distance' for abbreviation. As can be seen, λ is very large at $T < T_c$. We note that there is a small depression in the transition region. We will show below that this has important consequences on the spin current. We also note that at very low T ($T < 4$), λ suffers a decrease with decreasing T. This is a well-known artefact of MC simulation at very low T: the moving probability is so small that the motion of itinerant spins is somewhat slowed down. As we will show below when comparing with experimental data, this freezing is also observed in real systems due to finite experimental observation time.

Let us introduce now the definition of the mean free path. Let τ be the corresponding relaxation time; then the conductivity σ is proportional to τ: $\sigma = ne^2\tau/m$ according to the Drude theory (e: charge, m: mass). The resistivity $\rho(T) \equiv 1/\sigma$ is therefore inversely proportional to $\tau(T)$ by the relation $\rho(T) = \text{constant} \times (1/\tau(T))$. We can say that the resistivity is nothing but the number of collisions per time unit $1/\tau(T)$. Putting as the unit of resistivity $\rho(T = 0) = \text{constant} \times (1/\tau(T = 0)) = 1.0$, we can finally define the mean free path F as the mean distance in the x direction between two successive collisions, namely the distance λ divided by the number of collisions per time unit, i.e., by the resistivity as said earlier: $F(T) = \lambda(T)/\rho(T)/\rho(T = 0)$. Knowing $\rho(T)/\rho(T = 0)$ from the simulation, we can calculate $F(T)$. This is shown by the inset curve in figure 5. We see that the variation of F follows the variation of λ except close to T_c. In the following, for simplicity we shall present only λ because this quantity is directly related to the calculation of the spin resistivity.

Figures 6 and 7 show the effects of varying D_1 and D_2 at a low temperature $T = 1$. As seen in figure 6, λ is very large at small D_1: this can be explained by the fact that, for such small D_1, itinerant spins do not 'see' lattice spins in their interaction sphere so they move almost in

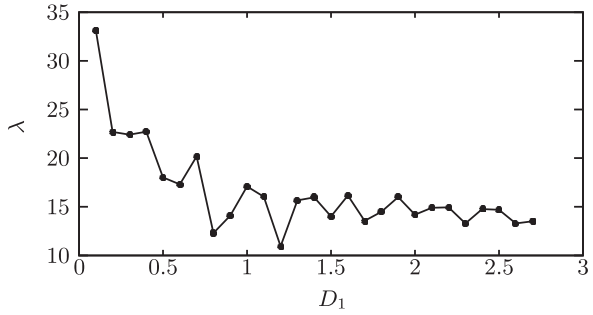

Figure 6. Characteristic distance λ versus D_1, at $T = 1$, $D_2 = 1$ and $E = 1$.

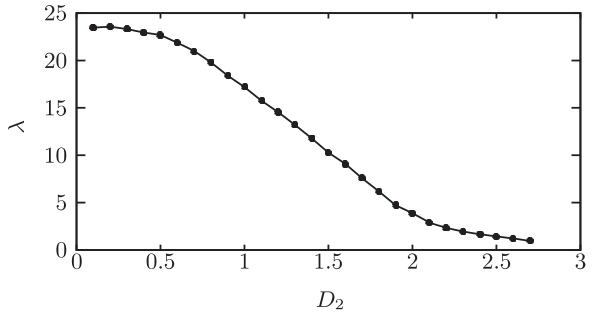

Figure 7. Characteristic distance λ versus D_2, at $T = 1$, $D_1 = 1$ and $E = 1$.

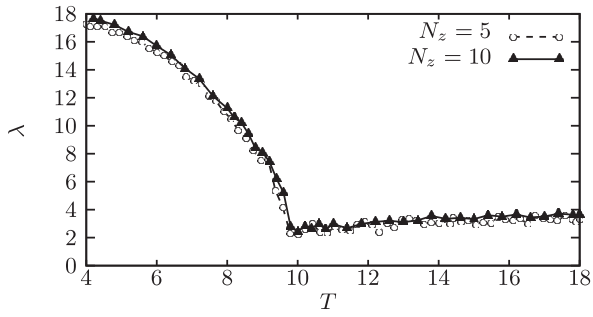

Figure 8. Characteristic distance λ versus T, for several thickness values of the magnetic film, with $D_1 = D_2 = 1$ and $E = 1$.

an empty space. The effect of D_2 is on the other hand qualitatively very different from that of D_1, as seen in figure 7: λ is saturated at small D_2 and decreases to the minimum value, namely $\lambda = 1$, at large D_2. We conclude that both D_1 and D_2 dominate λ at their small values. However, at large values, only D_2 has a strong effect on λ. This effect comes naturally from the criterion on the itinerant spin concentration used in the moving procedure.

The distance λ is shown in figure 8 as a function of T for two magnetic film thicknesses. In the absence of interface impurities, it is expected that there would be no large effects on the motion of itinerant spins. This is indeed what we observe here. Note however that λ for the smaller magnetic film thickness is systematically smaller than that of the thicker film. We will discuss on the role of interfaces below while showing the resistance (figure 11).

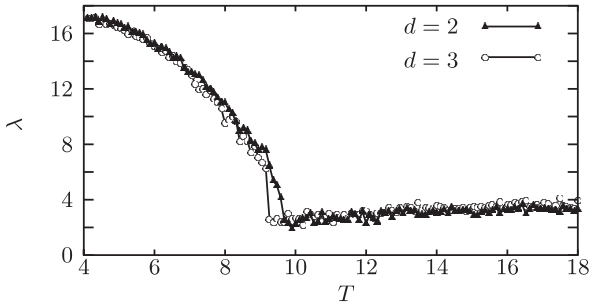

Figure 9. Characteristic distance λ versus T, for several spacer thicknesses with $D_1 = D_2 = 1$ and $E = 1$.

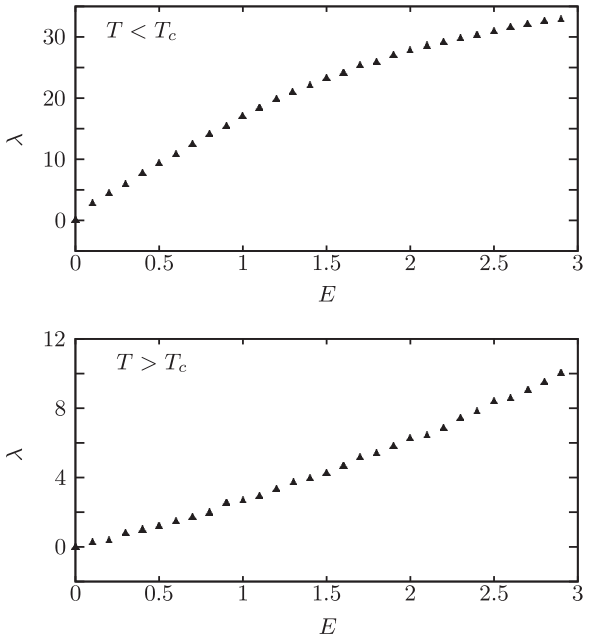

Figure 10. Characteristic distance λ versus E, below and above T_c, with $D_1 = D_2 = 1$.

We show in figure 9 the effect of the spacer thickness on λ. Note that for each thickness value we have used the inter film coupling constant J_i calculated by equation (2). Increasing the thickness, i.e., decreasing J_i, will result in a decrease of λ visible at low T, as can be seen in figure 9. This is expected since the itinerant spins at magnetic–non-magnetic interfaces have weaker inter-film coupling energy, so they are scattered more easily.

We show in figure 10 the effect of the electric field E for T both above and below T_c. The low-field part verifies the Ohm regime.

For the ith layer, we define the resistivity as

$$\rho_i = \frac{1}{n_i}, \tag{9}$$

where n_i is the number of spins crossing a unit area perpendicular to the x direction per unit of time. Note that this definition is applied to three magnetic layers ($i = 1, 3, 5$) and two

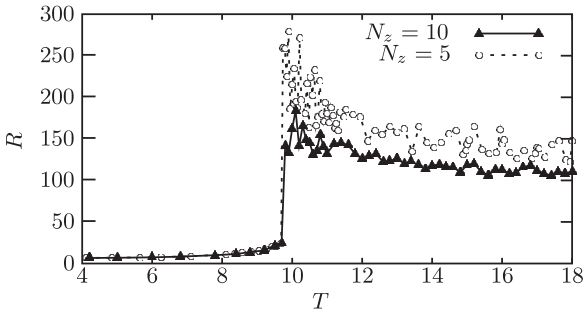

Figure 11. Resistance R in arbitrary units versus temperature T for two magnetic layer thicknesses.

non-magnetic layers ($i = 2, 4$). The total resistance R is defined as

$$R^{-1} = \sum_{i=1}^{5} \frac{1}{\rho_i}. \tag{10}$$

This definition is suitable for low-T phase where the spin current is distinct in magnitude between magnetic and non-magnetic layers. On the contrary, in the paramagnetic phase the spin current is almost spatially uniform, and the resistance can be defined as

$$R^{-1} = \frac{1}{\rho} = \frac{1}{5} \sum_{i=1}^{5} n_i. \tag{11}$$

In figure 11 we show the resistance R as a function of temperature.
There are several striking points:

- R is very low in the ordered phase and large in the paramagnetic phase. Below the transition temperature, there exists a single large cluster with small-sized excitation inside it (see figure 13), so that any itinerant spin having the appropriate orientation goes through the structure without any hindrance. The resistance is thus very small.
- R exhibits a cusp at the transition temperature, the existence of which was at first very surprising. While searching for its physical origin, we found that it was due to changes in the size distribution of clusters of lattice spins as the transition temperature is approached; it is known indeed from the theory of critical phenomena that clusters of up (respectively down) spins of every size form when T approaches T_c in a critical phase transition. At T_c, the distribution of cluster sizes displays clusters of various sizes, as can be seen from figure 12 (more details on the cluster construction algorithm will be given below). As a result, the conductivity is drastically lower than in the ordered phase since itinerant electrons have to steer around large clusters in order to go through the entire structure. Indeed, thermal fluctuations are still not large enough to allow the itinerant spin to overcome the energy barrier created by the opposite orientation of the clusters; this is all the more influential that we fixed an infinite spin-flip time, and this forbids the itinerant electron to reverse its orientation in order to reduce energy barriers. We will return to this point at the end of this section.
- Below T_c, there is no effect of magnetic layer thickness on R. However, for $T > T_c$, the larger thickness yields a smaller R. This can be explained by the effect of interfaces at non-magnetic spacers: near T_c the lattice spins at those interfaces are more strongly disordered than the bulk lattice spins, and they therefore enhance the resistance. The importance of

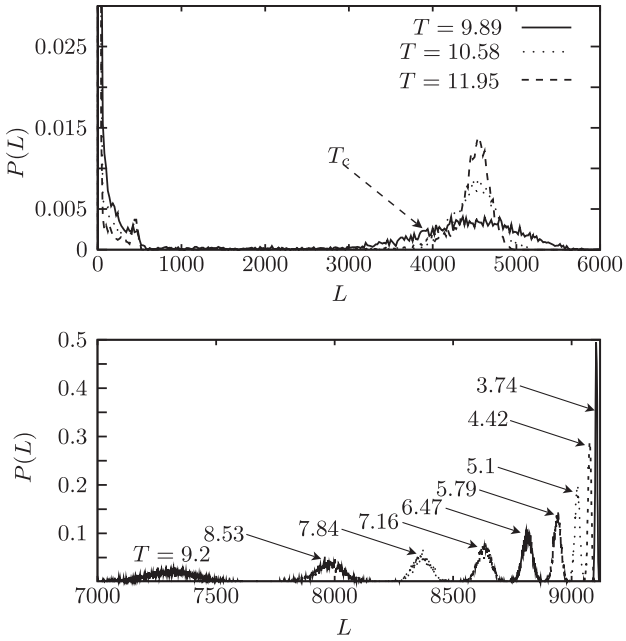

Figure 12. Distribution $P(L)$ of cluster size L at several temperatures T: (a) above T_c, (b) below T_c.

this contribution to the enhancement of the total resistance depends on the ratio of interface spins to bulk spins. This ratio becomes smaller when the magnetic layer thickness is larger.

Far above T_c, most clusters have a small size, so the resistivity is still quite large with respect to the low-T phase. However, a few facts account for the decrease of the resistivity as T is increased: (i) thermal fluctuations are now sufficient to help the itinerant spin overcome energy barriers that may occur when it bumps into islands of opposite orientation; (ii) the cluster size is now comparable with the radius D_1 of the interaction sphere, which in turns reduces the height of potential energy barriers.

We have tested this interpretation by first creating an artificial structure of alternate clusters of opposite spins and then injecting itinerant spins into the structure. We observed that itinerant spins do advance indeed more slowly than in the completely disordered phase (high-T paramagnetic phase). This finding is very interesting. We believe that it will have other important related physical effects yet to be discovered.

In order to show the existence of clusters at a given temperature, we have used the Kopelman algorithm to construct clusters [18]. We show in figure 12 the distribution of cluster size at different temperatures. As can be seen, the distribution peak is enlarged with increasing T.

We plot in figure 13(a) the cluster size A as a function of T. Figure 13(b) shows the ln–ln scale of A as a function of $T_c - T$. The slope is 0.094, indicating that A does not depend significantly on T at $T < T_c$, as expected.

At this stage, it is worth making a comparison with a recent experiment performed on a $Ni_{81}Fe_{19}/Al_2O_3$ multilayer by Brucas and Hanson [16]. This system is a magnetic permalloy/insulator multilayer which is very similar to our model: magnetic layers of thickness t (in the authors' notation) are separated by an insulator of fixed thickness of 16 Å. Measures

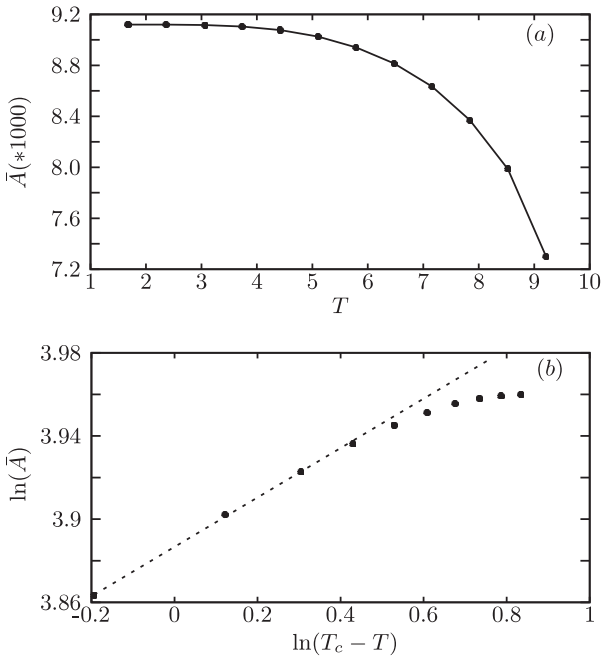

Figure 13. (*a*) Average cluster size versus T. (*b*) Average cluster size versus $(T_c - T)$ in the ln–ln scale.

of magnetization and resistance have been carried out as functions of T for two thicknesses $t = 16$ and 10 Å.

For $t = 16$ Å, x-ray reflectivity, transmission electron microscopy and Kerr measurements have shown that the magnetic layers are ferromagnetic with $T_c \simeq 225$ K. They found (see figure 2(a) of [16]) that the resistance is very small at low T (except for very low T), increases slowly with increasing T, makes a jump at T_c and saturates at room temperature, 300 K. This behaviour is very similar to what we obtained in the present study. We note however that our model gives a sharper jump than experimental data. This is due to the perfect crystalline structure (without impurities and defects) of our model, which is certainly not the case of the experimental system. Besides, at very low T (<25 K), due to thermally frozen dynamics, experimental measures show an anomaly also very similar to MC results at very low T: the decrease of λ with decreasing T shown in figure 5 at $T < 4$ means an increase of R with decreasing T. Both experimental and theoretical systems show therefore a long-relaxation effect due to finite observation time.

For $t = 10$ Å, the magnetic layers of the experimental system are in fact composed of superparamagnetic domains. In contrast to the case of $t = 16$ Å, the resistance in the case of $t = 10$ Å decreases with increasing T (see figure 2(b) of [16]). It is interesting to note that the experimental system in this case, which is composed of superparamagnetic domains, is equivalent to our model in the paramagnetic region above T_c, where the existence of domains of clusters is shown above. The behaviour of the resistance observed in our model for $T > T_c$ is in excellent agreement with experimental data (see figure 11 at $T > T_c$). The effect of domains on the resistance discovered in our present model is thus verified by this experiment.

Finally we show the effect of a magnetic field B applied in the z direction. If the inter-magnetic film coupling is $J_i = 1$, then, in the ground state, we need a critical field $B_c = 2$

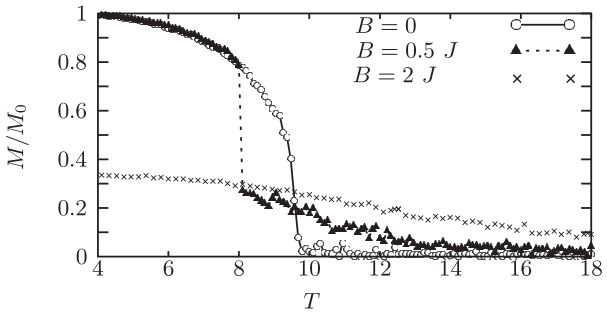

Figure 14. Staggered magnetization versus T for several B.

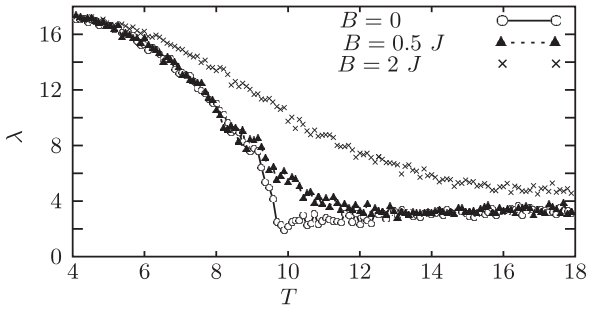

Figure 15. λ versus T for several values of B.

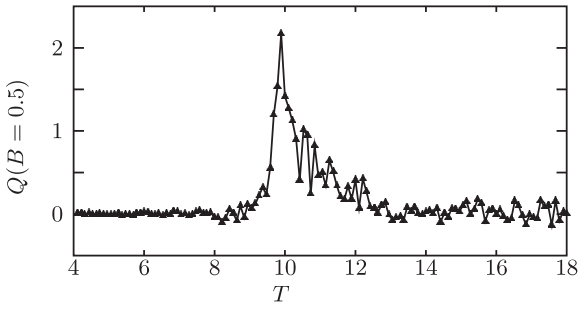

Figure 16. Magnetoresistance versus T for a low field $B = 0.5$. Note the peak at T slightly larger than T_c.

(in units of J) to align all spins in the z direction. We show in figure 14 the lattice staggered magnetization at $B = 0$, 0.5 and 2. As seen, for $B = 2$ all lattice spins are aligned in the z direction at low T: the staggered magnetization is then equal to $1/3$ at $T = 0$.

An applied field much smaller than B_c is expected not to modify significantly the itinerant spin current at $T \ll T_c$.

We show in figure 15 the characteristic length as a function of T for $B = 0$, 0.5 and 2. In order to show the effect of the magnetic field strength, we define the following quantity termed as 'magnetoresistance' hereafter:

$$Q(B) = \frac{\lambda(B) - \lambda(B = 0)}{\lambda(B = 0)}. \tag{12}$$

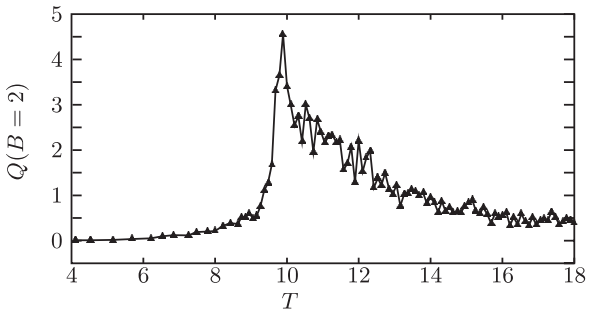

Figure 17. Magnetoresistance versus T for a large field $B = 2$. Note the peak is larger and higher than that observed in figure 16.

We now show in figure 16 the magnetoresistance in a weak field as a function of T. At low T, no significant magnetoresistance is expected since the itinerant spins are parallel to the lattice spins. The same is observed at T much larger than T_c: the lattice spins are parallel to the applied field, so the itinerant spins will go through the lattice without resistance. However, at T slightly larger than T_c we observe a large peak of the resistance. This peak has the same origin as that observed in figure 11, namely it is due to the existence of the structure of domains in the transition region.

For large fields, the same is observed except that the peak is wider and stronger as seen in figure 17 for $B = 2$.

Before the conclusion let us return to the two following points.

The first point concerns the effect of spin flip. The electron spin is not allowed to flip in this work because in doing so it will spend much more time on its trajectory and therefore will not contribute significantly to the final current. In fact if the spin is allowed to flip then it can go through an opposite spin cluster. However the total time needed for a spin to flip while going from one cluster to another is so large that it does not contribute to the final current, which is defined as the number of electrons crossing a unit area in a unit time (slow electrons do not contribute significantly). The cusp at T_c is, as a consequence, a little bit lower but the current intensity is much smaller as a whole.

The second point concerns the Ising model used here. We use this model not only for the sake of simplicity, aiming at finding a generic effect, but also for the fact that in very thin films experimental data show that perpendicular magnetic anisotropy takes place [11]. Of course, the discrete nature of the Ising spin exaggerates somewhat the jump of the resistance. If the spin has several components (Heisenberg model for instance), the jump would be more or less smoothened at T_c.

4. Concluding remarks

We have studied, by means of MC simulations, the transport of itinerant spins interacting with localized lattice spins in a trilayer system of FCC lattice structure in the CIP configuration. Various interactions have been taken into account. We found that the spin current is strongly dependent on the lattice spin ordering: at low T itinerant spins whose direction is parallel (antiparallel) to the lattice spins yield a strong (weak) current. At high temperatures, the lattice spins are disordered, and the current of itinerant spins is very weak and does not depend on the input orientation of itinerant spins. As a consequence, the resistance is very high at high T. We would like to emphasize here a striking effect found in the transition region between low-T

ordered phase and high-T paramagnetic phase: at T slightly higher than T_c, we discovered a peak of the resistance due to the existence of domains of lattice spins. Such an existence of domains in the critical temperature region is well known from the theory of critical phenomena, but no one has expected that it would play an important role in the spin transport. While writing this paper, we discovered an experimental paper that had just appeared [16], which supports our finding on the effect of domains in the resistance behaviour.

We have also investigated the effects on the spin current of different parameters which enter in our model: non-magnetic spacer thickness, interaction range, electric field, and magnetic field. The physical meaning of each of these effects has been discussed. Let us note that so far, except for reference [16], most magnetoresistance experiments have been performed as a function of an applied magnetic field, at a given temperature, while, in our present study, we have considered the effect of the lattice ordering on the spin current. We think that, in the light of the results obtained here, more experiments should be performed to investigate the effect of multilayer ordering on the spin transport.

As a final remark, we note that the CPP case is perhaps more difficult to study because effects from non-magnetic spacers as well as from impurities and roughness at interfaces will fully set in. Work is now in progress to study that case.

References

[1] Baibich M N, Broto J M, Fert A, Nguyen Van Dau F, Petroff F, Etienne P, Creuzet G, Friederich A and Chazelas J 1988 *Phys. Rev. Lett.* **61** 2472

[2] Grunberg P, Schreiber R, Pang Y, Brodsky M B and Sowers H 1986 *Phys. Rev. Lett.* **57** 2442
Binash G, Grunberg P, Saurenbach F and Zinn W 1989 *Phys. Rev.* B **39** 4828

[3] Barthélémy A *et al* 2002 *J. Magn. Magn. Mater.* **242–245** 68

[4] See review by Tsymbal E Y and Pettifor D G 2001 *Solid State Physics* vol 56 (San Diego, CA: Academic) pp 113–237

[5] Gravier L, Serrano-Guisan S, Reuse F and Ansermet J-P 2006 *Phys. Rev.* B **73** 024419

[6] Stewart D A, Butler W H, Zhang X-G and Los V F 2003 *Phys. Rev.* B **68** 014433

[7] Monchesky T L *et al* 2005 *Phys. Rev.* B **71** 214440

[8] McKenna K P, Michez L A, Morgan G J and Hickey B J 2005 *Phys. Rev.* B **72** 054418

[9] Carva K, Turek I, Kudrnovsky J and Bengone O 2006 *Phys. Rev.* B **73** 144421

[10] Zangwill A 1988 *Physics at Surfaces* (Cambridge: Cambridge University Press)

[11] Bland J A C and Heinrich B (ed) 1994 *Ultrathin Magnetic Structures* vol I and II (Berlin: Springer)

[12] Binder K 1983 *Phase Transitions and Critical Phenomena* vol 8, ed C Domb and J L Lebowitz (London: Academic)

[13] Diehl H W 1986 *Phase Transitions and Critical Phenomena* vol 10, ed C Domb and J L Lebowitz (London: Academic)
Diehl H W 1997 *Int. J. Mod. Phys.* B **11** 3503

[14] Thanh Ngo V, Viet Nguyen H, Diep H T and Lien Nguyen V 2004 *Phys. Rev.* B **69** 134429

[15] Thanh Ngo V and Diep H T 2007 *Phys. Rev.* B **75** 035412 and references on surface effects cited therein

[16] Brucas R and Hanson M 2007 *J. Magn. Magn. Mater.* **310** 2521

[17] Binder K and Heermann D W 1988 *Monte Carlo Simulation in Statistical Physics* (New York: Springer)

[18] Hoshen J and Kopelman R 1974 *Phys. Rev.* B **14** 3438